Seismic Images of the Far Side of the Sun

C. Lindsey[1*] and D. C. Braun[1,2]

Images of an active region on the far side of the Sun were derived by applying seismic holography to recent helioseismic observations from space. Active regions are the centers of energetic phenomena such as solar flares and coronal mass ejections whose resulting electromagnetic and particle radiation interfere with telecommunications and power transmissions on Earth and can pose significant hazards to astronauts and spacecraft. Synoptic seismic imaging of far-side solar activity will now allow us to anticipate the appearance of large active regions more than a week ahead of their arrival on the east solar limb.

Forecasts of space weather would be greatly improved by the ability to monitor active regions on the far side of the Sun. Active regions on the near solar surface produce flares that affect spacecraft, cause surges in electrical power grids, and inhibit telecommunications. Because the Sun rotates rapidly, with a synodic period of 27 days, flaring regions can appear suddenly on the east solar limb to affect space weather in the terrestrial neighborhood as they pass across the near solar surface. Many such regions could be anticipated by a week or more if we could effectively monitor the far surface of the Sun.

Helioseismic holography was proposed a decade ago (1) as a general diagnostic basis for local helioseismology, with the purpose of imaging of local acoustic anomalies in the solar interior and on the far side. The development of holographic seismic imaging techniques for solar interior diagnostics (2,3) was initially prompted by the discovery that sunspots absorb (4,5) and scatter (6) incident acoustic waves. Phase-coherent seismic imaging opened not only the possibility of detecting local magnetic and thermal structure beneath the solar surface, but even active regions on the far side of the Sun (1). These techniques work because the solar interior is transparent to seismic waves. We developed the basic concepts for seismic holography for these purposes (1,2,7), reviving a concept originally proposed some 15 years earlier by Roddier (8).

Standard holographic imaging of the near solar interior is accomplished computationally by regressing surface acoustic wave disturbances, determined by helioseismic observations, backwards into the interior, based on a computational acoustic model of the solar interior (9), thereby to express a field called the coherent acoustic egression, H_+ (10). Generally, the surface observations that contribute to the regressed acoustic field at any given

[1]Solar Physics Research Corporation, Tucson, Arizona 85718, USA. [2]NorthWest Research Associates Inc., Colorado Research Associates Division, Boulder, Colorado 80301, USA.

[*]To whom correspondence should be addressed. E-mail: lindsey@sprc.com.

"focal point" in the image are chosen from a limited region, called the pupil of the computation. This has typically been an annulus or circular region on the model surface centered directly above the submerged focal point. In fact, waves in the 2.5–4.5 mHz frequency range undergo a specular reflection at the solar surface, penetrating back into the interior where they are eventually refracted back to the surface thousands of km further from the source. Multiple-skip holography based on this phenomenon thus facilitates imaging of active regions with pupils far extended from the focal point. Indeed, it is even possible to extend the pupil of a holographic computation from the focal point to the opposite side of the Sun. In such an application, it is the focal point that must lie on the far surface of the Sun, since the pupil itself must lie on the near surface in order to be directly observed. This is the principle of far-side helioseismic holography.

Standard acoustic power holography is accomplished by mapping the egression power, $|H_+|^2$, which may be integrated over time and/or temporal frequency for improved statistics. This diagnostic is sensitive to acoustic sources and absorbers, the latter of which are rendered as silhouettes. Alternatively, phase-sensitive holography (7) can be used to gauge travel-time perturbations, Δt, caused by refractive anomalies, or the magnetic depressions of sunspots and plages (11). This technique is based on phase correlations between the acoustic egression and its time-reverse counterpart, the acoustic ingression, H_-, which is a coherent representation of waves that happen to be converging into the focal point, as opposed to waves emanating from it. This is the natural adaptation of time-distance correlation measurements (12,13) to holographic reconstruction.

Here, we used two-skip phase-sensitive holography to map travel-time perturbations of the far side of the Sun over the spectral range 2.5–4.5 mHz. We analyzed a 24-hour interval of full-disk Dopplergrams starting on 28 March 1998 07:00 UT, made by the Solar Oscillations Investigation-Michelson Doppler Imager (SOI-MDI) aboard the Solar Heliospheric Observatory (*SOHO*) spacecraft (14). We computed two-skip egression and ingression maps over the spectral range 2.5–4.5 mHz using a near-side pupil spanning a range from 115°–172° from the focal point (Fig. 1). Such a configuration effectively filters the egression computation for waves whose spherical harmonic indices, ℓ, are mostly confined to a well-defined range (15). At 3.5 mHz, for example, the pupil illustrated in Fig. 1 samples waves with ℓ predominantly in the range 22–40. This imposes a diffraction limit of $\sim$10° of longitude at the solar equator, easily resolving a moderately large plage. The computations made here were devised to image an area on the solar far side that included a large, multipolar magnetic region, NOAA AR 8194 (16), which we reference to Carrington longitude 29.8° and latitude −22.8°, about 18 hr before its passage through the far-side meridian. The result is a signature that renders the active region on the far

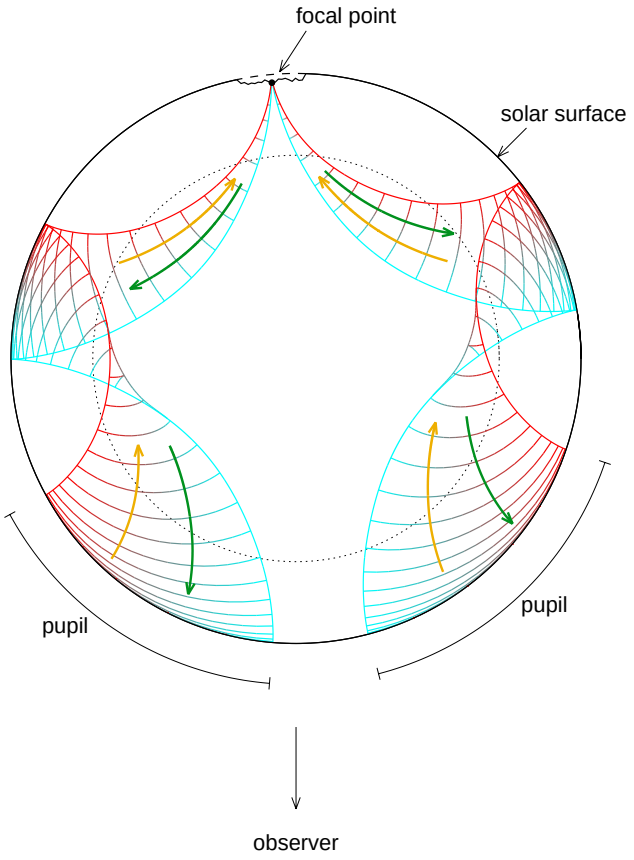

Fig. 1. Cross-section of the solar interior showing the wave configuration for two-skip far-side seismic holography. Wavefronts emanating from a far-side point source (focal point) at intervals of 286 sec (1/3.5 mHz) within the corridor of trajectories shown reflect once from the solar surface (right and left sides) and arrive in an annular pupil on the near surface (bottom) of the Sun. Waves coherently emanating from the focal point (green arrows) are represented by the acoustic egression, reconstructed for each focal point in the image from the surface disturbance it creates on the near surface. Its time reverse signature, the ingression (yellow arrows), represents identical waves coherently converging into the focal point to contribute to the local disturbance there. A local acoustic depression at the focal point will shift the phase of the ingression-egression correlation. In the case of a quasi-specular reflection at the focal point, the outside of the ingression pupil on one side (red part of wavefronts) correlates with the outside of the ingression pupil on the other (also red). Likewise for the inside of the pupil (cyan part of wavefronts). Thus, the loss of either side of the pupil destroys the phase correlation for the entire pupil. For this reason, phase-sensitive holography of far-side solar activity is only practical for regions within approximately 50° of the antipode of disk center. The dotted circle indicates the depth of the base of the solar convection zone.

side of the Sun by a local reduction in the one-way sound-travel time of about 6 sec over an area covering about 300 degree^2 (Fig. 2A). This is consistent with the sign and magnitude of signatures that typically characterize plages imaged on the near side (17) of the Sun.

When the foregoing computation is repeated over the 24 hr interval beginning 29 March 1998 10:40 UT, centered at the same Carrington coordinates so as to follow solar rotation, then the signature recurs (Fig. 2B). During this time the region passed through the far-side meridian, and appears to have been growing rapidly. The NSO/Kitt Peak magnetogram (18) of 08 April 1998, projected onto the same Carrington coordinates as the sound-travel-time maps, shows the magnetic region 10 days later, now on the near side of the Sun just inside of the east limb (Fig. 2C).

The seismic imaging of the far side of the Sun has important implications for research on the acoustic properties of magnetic regions and of the Sun as a whole. The far-side images directly demonstrate the influence of active regions on global modes. Because these waves travel from the near side of the Sun to the far side and back, they interfere with their multiple reflections. The result is a standing wave with a sharply defined frequency, called a p-mode, similar to the harmonics that resonate in an organ pipe. An active region can be likened to a subtle dent in the organ pipe, slightly reducing its internal volume and thereby slightly raising its resonant frequency. As in the organ pipe, the resonant frequencies of solar p-modes can essentially be regarded as independent of which side of the resonant cavity the active region is on. Thus, the same acoustic perturbations that are largely, perhaps entirely, responsible for shifting the resonant frequencies of solar p-modes locate active regions on the far side of the Sun when these modes are treated from the local optical perspective of seismic holography. The far-side images therefore reinforce a growing consensus (19,20) that reduced sound travel times in active regions may explain the entirety of the frequency shifts of global p-modes with the solar cycle.

The application of seismic holography to active regions on the far side of the Sun makes it possible to study how active regions absorb, emit and scatter low-ℓ waves. Plain acoustic power holography of near-side active regions renders both sunspots and plage with strong egression power deficits, comparable in significance to the phase shifts. Acoustic power holography of far-side active regions renders an unexpectedly weak signature, not clearly detectable in our computations. We therefore see that the deficit in acoustic noise radiating from plages (6,21,22) is substantially selective in favor of high-ℓ p-modes. This remarkable development seems tentatively consistent with recent work that attributes the acoustic egression deficit of waves emanating from magnetic regions to the coupling of p-modes with slow Alfvèn modes (23,24). Low-ℓ p-modes are characterized by mostly vertical motion, and therefore couple only weakly to magnetic fields that are vertical.

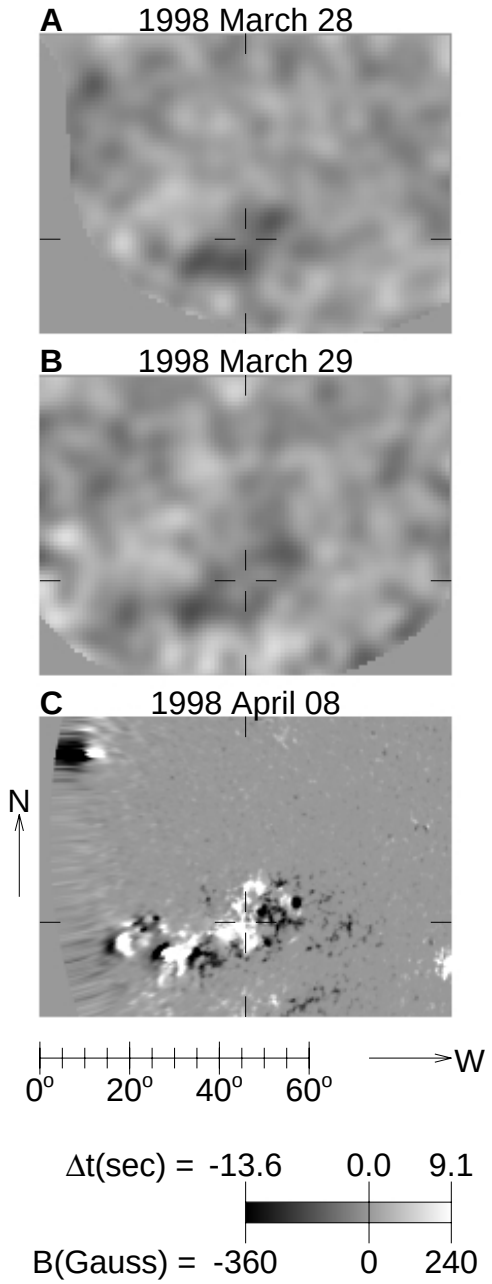

Fig. 2 Maps of one-way sound travel-time perturbation, Δt, in the neighborhood of NOAA AR 8194 just before (**A**) and during (**B**) its passage through the far-side solar meridian. Vertical fiducials in the center of each frame mark Carrington longitude $29.78°$. Horizontal fiducials cross that meridian at solar latitude $-22.82°$. (**C**) an NSO/Kitt Peak magnetogram of the same location a week and a half later, as the magnetic region becomes visible just inside of the east limb. All three maps are overhead-view Postel projections centered on the above reference location with radial distance from the reference point indicated by the rule just beneath the bottom frame.

References and Notes

1. C. Lindsey and D. C. Braun, *Solar Phys.* **126**, 101 (1990).
2. D. C. Braun, C. Lindsey, Y. Fan, S. M. Jefferies, *Astrophys. J.* **392**, 739 (1992).
3. C. Lindsey, D. C. Braun, S. M. Jefferies in *GONG 1992: Seismic Investigation of the Sun and Stars* (Astronomical Society of the Pacific, San Francisco, 1993) p. 81.
4. D. C. Braun, T. L. Duvall Jr., B. J. LaBonte, *Astrophys. J.* **335**, 1015 (1988).
5. T. J. Bogdan, T. M. Brown, B. W. Lites, J. H. Thomas, *Astrophys. J.* **406**, 723 (1993).
6. D. C. Braun, *Astrophys. J.* **451**, 859 (1995).
7. C. Lindsey and D. C. Braun, *Astrophys. J.* **485**, 895 (1997).
8. F. Roddier, *Compt. Rend. Accad. Sci.* **281**, B993 (1975).
9. J. Christensen-Dalsgaard, C. R. Proffitt, M. J. Thompson, *Astrophys. J.* **403**, L75, 1993.
10. C. Lindsey and D. C. Braun, *Solar Phys.*, (in press) see §3, equation (1).
11. Plages are magnetic regions whose flux densities, ranging from 100–1,200 G are considerably greater than those of the quiet Sun (± 100 G) but considerably less those of sunspots (2–3,000 G). Plages viewed near the center of the solar disk are nearly invisible against the quiet Sun in white light, but near the limb are about 5% brighter than the quiet Sun. The strong magnetic fields of sunspots visibly depress their umbrae more than 200 km beneath level of the quiet photosphere. The reduced travel times of plages may be the result of a similar, but smaller, depression by their weaker magnetic fields.
12. T. L. Duvall Jr., S. M. Jefferies, J. W. Harvey, M. A. Pomerantz, *Nature* **362**, 430 (1993).
13. T. L. Duvall Jr, S. D'Silva, S. M. Jefferies, J. W. Harvey, J. Schou, *Nature* **379**, 235 (1996).
14. P. H. Scherrer, *et al.*, *Solar Phys.* **162**, 129 (1995).
15. C. Lindsey and D. C. Braun, *Solar Phys.*, (submitted) see §4.
16. The National Oceanic and Atmospheric Administration (NOAA), a branch of the US Department of Commerce, monitors solar activity, assigning numbers to each major sunspot group. These are published in a periodical, *Solar Geophysical Data*, printed monthly by NOAA.
17. D. C. Braun, and C. Lindsey, *Solar Phys.*, (in press).
18. The National Solar Observatory (NSO) operates solar telescopes at the Kitt Peak National Observatory near Tucson, Arizona and at the Sacramento Peak Observatory, near Cloudcroft, New Mexico. NSO runs a synoptic program at the Kitt Peak Vacuum Telescope that provides daily magnetograms covering the full solar hemisphere that is directly visible from the Earth. These are made available on the websites http://www.nso.noao.edu/dataarch.html and http://argo.tuc.noao.edu/synoptic/synoptic.html.
19. R. Howe, R. Komm, F. Hill 1999 *Ap. J.* **524**, 1084.
20. B. W. Hindman, D. A. Haber, J. Toomre, R. Bogart 2000, *Solar Phys.* (submitted).
21. C. Lindsey and D. C. Braun, *Astrophys. J.* **499**, L99 (1998).
22. D. C. Braun, C. Lindsey, Y. Fan, M. Fagan, *Astrophys. J.* **502**, 968 (1998).
23. Cally, P. S., & Bogdan, T. J. 1997, *Ap. J.* **486**, L67.
24. Cally, P. S. 2000, *Solar Phys.* (in press).

25. We greatly appreciate the support we have gotten from Dr. P. Scherrer, and early and enthusiastic proponent of far-side imaging, and of the *SOHO* SOI-MDI team. *SOHO* is a project of international cooperation between ESA and NASA. This work has been supported by NSF Grants ATM-9214714 and AST-9528249, by NASA Grant NAG5-7236, and by a research contract, PY-0184, sponsored by Stanford University.

Supplementary Material

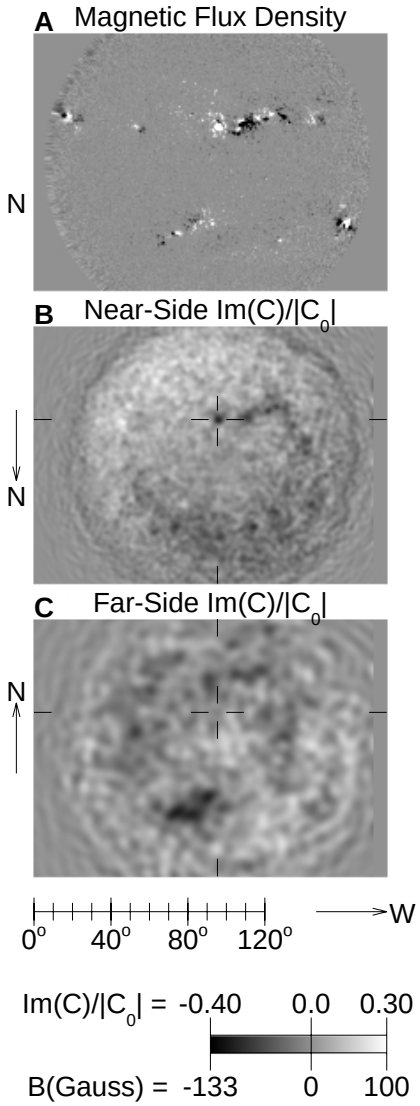

Supplemental Fig. 1. Comparative phase-correlation maps of the near side and far side of the Sun show that far-side images are not substantially contaminated by near-side artifacts. A *SOHO*-MDI magnetogram on 28 March 1998 (**A**) is compared with the imaginary part of the correlation, $C(\mathbf{r},\nu) = \langle H_{-}(\mathbf{r},\nu)\ H_{+}^{*}(\mathbf{r},\nu)\rangle$ focused on the near side of the Sun (**B**) and the far side (**C**).

The correlations, C, in the foregoing Figure are normalized to $|C|$ at disk center. The near-side images (**A** and **B**) are flipped about the horizontal axis through disk center, so that Carrington north is towards the bottom of the page. This way, each pixel in either near-side image matches the location of its antipode in the far-side image (**C**). Fiducials mark the position of a sunspot in NOAA AR 8185 in **A** and **B** and its antipode in **C**. Extending $\sim$28° west (right) and slightly south (above) AR 8185 in the near-side images is AR 8189. Near-side seismic images may show significant features that do not appear in magnetograms. An example is the conspicuous finger extending some 25° north-west (below and to the right) of the western (right) limit of AR 8189 in **B**. This may be the signature of a near-side but subsurface acoustic anomaly. However, we have yet to see any evidence that holographic computations focused on the surface of the Sun render significant artifacts of any kind in computations focused on the far side. Nor have we found any basis on which to expect any such artifacts.

Diffraction and Spatial Discrimination. Solar p-modes are characterized by a spherical harmonic index, ℓ, roughly related to their surface wavelengths,

$$\lambda = 2\pi R_\odot/\ell,$$

where $R_\odot$ is the solar radius. Holographic computations that sample waves up to a particular index, ℓ, generally render images whose diffraction-limited resolution is approxmately λ. For a given frequency, ν, the waves with lower ℓ are those directed along deeper trajectories. These are the waves whose paths span the greatest distance in a single skip before returning to the surface. If $R_{\rm min}$ is the minimum radius to which the ray path penetrates before returning towards the surface, then

$$\ell = \frac{R_{\rm min}\nu}{c_{\rm min}},$$

where $c_{\rm min}$ is the speed of sound at depth $R_{\rm min}$. In simple, single-skip holography of a source near the surface, the more extended pupils sample waves that have skipped a great distance, those with lower ℓ, which render the poorer spatial resolution in terms of diffraction. Double-skip holography allows the analyst to double the extension of the pupil and enjoy the same resolution.